





A New Communication-Free Dual Setting Protection Coordination of Microgrid

Heba Beder , Baraa Mohandes , *Member, IEEE*, Mohamed Shawky El Moursi , *Senior Member, IEEE*, Ebrahim A. Badran , *Member, IEEE*, and Magdi M. El Saadawi

Abstract—Protection coordination for the microgrid system in both islanded and grid connected modes is considered a challenge for microgrid operation. The variation in short circuit currents in each mode of operation, limitation of protection curves in the relays, and the need for fast and reliable communication are the main challenges tackled in research. Direction overcurrent relays are considered the main protection instrument for the microgrid. However, one protection setting for both (main and backup) operation does not provide a fast-operating time. On the contrary, the dependence on communication to maintain the proper backup protection operation is not a reliable solution for protection system. Therefore, this paper introduces a fast, reliable, and simple protection scheme for secure microgrid operation in both islanded and grid connected modes. In this context, one set of protection settings is optimized and used in both modes of operation. A protection setting consists of two time-dial settings and one pickup current setting for each relay. The proposed design technique minimizes the total operating time for both main and backup relays. As all protection functions are executed in the forward direction, no communication is needed among relays. The proposed scheme is tested and verified on a modified portion of IEEE 30 bus test system equipped with distributed generation units. A comparative analysis is carried out and the results demonstrate superior performance by the proposed scheme in comparison with the dual setting scheme with communication.

Index Terms—Microgrids, directional overcurrent relays, optimal protection coordination, distributed generation.

I. INTRODUCTION

THE microgrid concept is a potential solution for the growing demand problem [1]. The reliability factor is important

Manuscript received March 19, 2020; revised July 30, 2020 and September 30, 2020; accepted November 14, 2020. Date of publication December 8, 2020; date of current version July 23, 2021. This work was supported by the Khalifa University of Science and Technology under Award No. CIRA-2018-37. Paper no. TPWRD-00416-2020. (*Corresponding author: Mohamed Shawky El Moursi.*)

Heba Beder is with the North Delta Electricity Distribution Company, Mansoura 35511, Egypt (e-mail: hebabeder78@gmail.com).

Baraa Mohandes is with the Electrical Engineering and Computer Science Department, Khalifa University, Abu Dhabi 127788, United Arab Emirates (e-mail: mohamed.elmoursi@ku.ac.ae).

Mohamed Shawky El Moursi is with the Advanced Power and Energy Center (APEC), Department of Electrical Engineering and Computer Science, Khalifa University, Abu Dhabi 127788, United Arab Emirates. He is currently on leave from the Faculty of Engineering, Mansoura University, Mansoura 35516, Egypt (e-mail: melmoursi@masdar.ac.ae).

Ebrahim A. Badran and Magdi M. El Saadawi are with the Electrical Engineering Department, Faculty of Engineering, Mansoura University, Mansoura 35516, Egypt (e-mail: ebadran@mans.edu.eg; m_saadawi@mans.edu.eg).

Color versions of one or more of the figures in this article are available at <https://doi.org/10.1109/TPWRD.2020.3041753>.

Digital Object Identifier 10.1109/TPWRD.2020.3041753

for encouraging the investments in microgrid. Stable operation and robust protection system are essential for microgrid's reliability [2]. The microgrid's different modes of operation (grid connected and islanded) create a variety of fault scenarios which affects the protection system's selectivity, sensitivity and speed [3]–[5]. The Direction Over Current Relay (DOCR) is one of the main microgrid protection components [6]. Many optimization methods are introduced to find the optimal setting of the DOCR with or without fault current limiter in different constraints and modes of operation, in order to minimize the relays operating time [7]–[13]. The limited number of industrial protection characteristic curves restrains the optimization algorithms ability to find fast operating time for high fault current resulted from grid connected microgrid [14]–[17]. On the other hand, the majority of literature assigns a single protection setting for both main and backup operation in a relay. Consequently, it slows the relays' operating time since one optimization constraint at least from several constraints needs to be released [18]. Some studies deal with these two issues.

The first issue is the limited number of available standard protection curves. The second issue is the need to release one optimization constraint. The first issue is investigated in [14]–[17], and a solution based on a new tripping current characteristic for DOCRs is introduced. In [15], a new Time Current- Voltage (TCV) characteristic for DOCR is introduced considering an additional term in the time current characteristic equation to represent the relationship between the fault's voltage (voltage dip) and the relay operating time. The optimization technique is used to tune the additional term to achieve proper protection coordination accordingly. Although the method reduces the operating time compared to the conventional method, the obtained operating time is long for the studied maximum fault current.

The relation between the high fault current resulting from DG integration and the fixed point of maximum Current Multiplier Setting (CMS) in the industrial relays is discussed in [14]. The relays fault current may increase beyond this point, which results in a fixed operating time for a variant high fault current. The reference proposed a non-standard characteristic curve by adding a new CMS maximum constraint into the optimization problem. The scheme succeeded in different DG location for both grid connected and islanded operation of the microgrid to maintain the coordination between relays. The results show that the maximum fault current experienced by the relays does not exceed the new proposed CMS, leading to improved relays operating time. However, this improvement is

insignificant compared to the high fault current resulting from the studied three phase fault. In [16], an auxiliary variable was added to the classical operation time model of each DOCR to reduce the relays operating time. The proposed auxiliary variable shifts the protection curve vertically in order to adjust the relays operating time. After that, the auxiliary variable is added as a constraint in the optimization model, which creates a new Tripping Characteristic Curve (TCC). The protection strategy is tested and proven superior to the conventional optimization method and the user defined coordination method. Despite the obtained tripping time of primary protection relays is short in most cases, it is slow in cases of faults at the far end of a line.

In [17], a new characteristic curve is proposed with the objective of reducing the energy dissipated in the fault. The protection scheme is tested in a radial system, and it is compared with the conventional scheme. However, more investigation for applications in meshed system are required. For the previous investigated method, i.e., new TCC, it is found that employing one protection curve for both primary and backup protection is not optimal. Although it yields fast primary protection operation, the backup protection operation is very slow for the same fault. For the second issue (i.e., the need to relax one optimization constraint), this issue is tackled in [18]–[23]. The authors investigate a dual protection setting for DOCR, where each setting works in different direction: one for primary protection in forward direction and the second one backup protection in reverse direction. This method requires a communication infrastructure for effective backup relays operation.

In [18], a technique is adopted and verified in both islanded and grid connected modes for the microgrid. This method was an extension work for [19]. In [20], the dual setting method has been developed to cope with the radial system topology, and the transient stability for the connected DGs are considered. Ref. [21] introduced a comparison between conventional optimization coordination and a dual setting optimization in case of different relay characteristics from the IEC standard. It is concluded that the dual setting saves total relays operating time in different characteristics. However, it didn't represent the detailed relays operating time. In [22] the dual setting principle considering multiple fault location is represented. Despite the fact that the dual setting protection scheme reduces total relays operating time, this improvement decays with wide-spread implementation of this scheme. At the same time, replacing all DOCRs with dual setting relays incurs additional costs [23]. Ref. [23] proposed a techno-economic distribution for dual setting relays in meshed distribution system in order to minimize total operating time. In addition, non-standard inverse characteristic curve is optimized for that dual setting relays. This technique is considered as the first research that combines both techniques, non-standard inverse curve besides the dual settings. However, the relays operating time in primary and backup modes are relatively slow with respect to the high three-phase fault current in some scenarios.

Although the relays operating time is better than that of the conventional method, the reduction in operating time, for both primary and backup protection, however this is insignificant in comparison with the increase in the three-phase fault current

level. In addition, the method requires communication among relays, which introduces new risk factors such as communication link failures and cyber intrusions [24].

In this paper, a new and simple dual protection settings is introduced. Both of the dual settings work in the forward direction, and without any communication among relays. The first setting of a relay is the primary protection's TDS, which based on the very inverse curve. The second setting of the same relay is the TDS for backup protection, based on the normal inverse curve. The main contributions of the proposed protection technique are:

- A novel approach to the dual setting scheme that provides faster operating time especially for primary protection.
- Operating the backup relays work in forward direction, and thus, no communication link is required for proper backup coordination. This increases the protection's reliability and resilience against cyber threats.
- The protection curves are taken from the industrial characteristics' curves; very inverse and inverse curve. The method does not require new relay characteristics.
- Adopting the very inverse curve for the primary protection setting, which is characterized by fast tripping action. This contributes much faster operation with respect to higher fault currents brought by higher penetration of distributed generation.
- The backup setting employs the normal inverse curve, providing a reasonable backup operating time, especially for a lower fault current value.

The settings are optimized and tested for a portion of the IEEE 30 bus test system. Furthermore, the results are compared with the traditional dual setting scheme presented in [18] and the improvement in the total operating time are demonstrated. In addition, the minimum coordination interval between relays is preserved, thus, demonstrating the advantages of the proposed method.

II. PROPOSED PROTECTION COORDINATION ALGORITHM

The objective function of the protection coordination design is to minimize the total relays clearing time for faults. The design problem can be modeled as linear or non-linear optimization problem [18]. Different optimization tools are commonly used to solve the protection coordination problem. The decision variables of the optimization model are the settings of each relay: The Time Dial Setting (TDS) in primary protection mode and backup protection mode, and the pickup current (I_p). Hence, the objective function is expressed as follows:

$$\min_{\{TDS_i^{pm}, TDS_i^{bk}, I_{p,i}\}} T = \sum^{(c,i,j)} \left(t_i^{pm} (I_{SC,j,c}) + \sum_{k=0}^K t_i^{bk} (I_{SC,k,c}) \right) \quad (1)$$

Subject to, the operating time of the inverse curve:

$$t_{ij} = TDS_i \frac{A}{\left(\frac{I_{SCij}}{I_{p,i}} \right)^B - 1} \quad (2)$$

TABLE I
TRIPPING CURVE CHARACTERISTIC COEFFICIENTS [25]

	Very Inverse (Primary Protection)	Normal Inverse (Backup)
A	13.5	0.14
B	1	0.02

where I_{sc} is the short circuit current pass through relay i . The superscript i is the relay index, j is the fault location index, k is the number of backup relays, pm identifies primary protection relays, and b identifies the backup relays. Subscript c distinguishes between faults occurring while the microgrid is in grid-connected mode versus operating in islanded mode.

Eq. (1) represents the optimization's objective function, which is minimizing the total operating time for all the primary relays and their backup relays. Eq. (2) is the generic expression of relay operating time for different inverse overcurrent characteristics. t_{ij} is the relay operating time for relay i and fault location at j . A and B are coefficients of the tripping curve, whose values are given in Table I [25]. The very-inverse tripping curve is used in the primary protection mode in all relays, while the normal-inverse tripping curve is used for the backup protection mode.

The objective function should accomplish the following constraints in both modes of operation (grid-connected and islanded).

$$t_i^{bk}(I_{SC,j,c}) - t_i^{pm}(I_{SC,j,c}) \geq CTI, \forall i, j \quad (3)$$

Where CTI is the minimum coordination interval required to discriminate between primary relay operating time t_i^{pm} and backup relay operating time t_i^{bk} for the same fault location. Therefore, CTI must take a value between (0.2–0.5) sec [11]. A CTI value of 0.2s is adopted in this paper.

The pickup current setting of a relay is designed according to Eq. (4), which ensures that it is larger than the maximum load current in its zone. At the same time, the pickup current must be smaller than the minimum fault current seen by relay in backup mode.

$$1.1 \cdot I_{L,i} \leq I_{p,i} \leq a \cdot I_{SC,j} \quad (4)$$

$$a = \begin{cases} 60\% & \text{if } 60\% \cdot I_{SC,j} \geq 1.1 \cdot I_{L,i} \\ 80\% & \text{otherwise} \end{cases}$$

where $I_{L,i}$ is the maximum load current in relay i , $I_{p,i}$ is the pickup current setting of relay i in p.u. It is important to note that there is only one pickup current value setting for both primary and backup protection modes.

$$TDS_{\min} \leq TDS_i^{bk} \leq TDS_{\max} \quad (5)$$

$$TDS_{\min} \leq TDS_i^{pm} \leq TDS_{\max} \quad (6)$$

TDS_i^{pm} , TDS_i^{bk} are the Time Dial Setting of relay i in primary protection mode and backup protection mode, respectively. TDS_{\max} and TDS_{\min} in (5), and (6) are the upper and lower limits of a relay's TDS. These limits are the relay manufacturer settings [25], TDS_{\min} and TDS_{\max} values are selected to be 0.05 and 0.35.

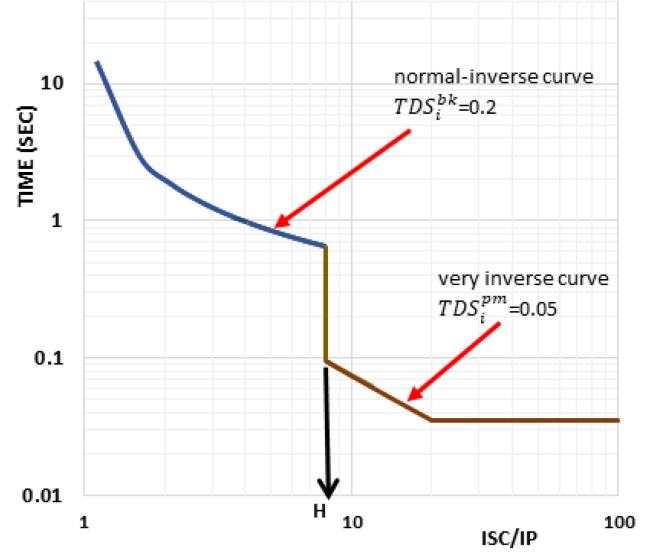


Fig. 1. The proposed protection characteristic curves.

Eq. (7) describes the novel coordination criterion of this paper. That is, the tripping time in primary protection mode for every relay should always be less than the tripping time in backup protection mode. Point (H) is the point of discontinuity in the protection curve, lying at the maximum possible fault current seen in the backup protection mode, and at the minimum possible fault current observed in primary protection mode. If the fault current measured by the relay is equal to or greater than the value H, the relay operates in primary protection mode with the very-inverse curve. Otherwise, the relay operates according to the backup setting with normal-inverse curve. Fig. 1 represents the proposed protection characteristic curve for the direction over current relay for both primary and backup operation mode.

$$t_i^{bk}(H) \geq t_i^{pm}(H) \quad (7)$$

In Fig. 1, the proposed protection characteristic curve combines the normal-inverse curve for (backup setting) and very inverse curve for (primary setting) in one operating curve. This hybrid curve works in forward direction. Point (H) defines the end of the normal inverse curve (for backup setting) and the start point of the very inverse curve (for primary setting). Employing the very inverse curve ensures very fast operating time in primary mode, while the normal-inverse curve provides relatively fast operation in backup mode with respect to CTI. Eq. (8) describes the curve for relay i .

$$t_{op} = \begin{cases} \left(TDS_b \frac{0.14}{(\tilde{I})^{0.02-1}} \right) & \text{for } \{1.1 \leq \tilde{I} < H\} \\ \text{backup setting} & \\ \left(TDS_{pm} \frac{13.5}{(\tilde{I})^{1-1}} \right) & \text{for } \{H \leq \tilde{I} \leq 100\} \\ \text{primary setting} & \end{cases} \quad (8)$$

$$t_i^{pm} \leq 0.15s, t_i^{bk} \leq 0.75s \quad (9)$$

$$\tilde{I} = \begin{cases} I_{SC}/I_p & I_{SC}/I_p \leq I_{CT}^{\max} \\ I_{CT}^{\max} & I_{SC}/I_p > I_{CT}^{\max} \end{cases} \quad (10)$$

where t_{op} is the relay i operating time, \tilde{I} is I_{sc}/I_P , and H is the fault current value in case of minimum phase fault in the primary relay over the pickup current. I_{CT}^{max} is the saturation current of the relay's current transformer.

Eq. (10) represents the effect of current transformer saturation on (9) whereas the current-transformer core applies a cap on the maximum fault current measured by the relay. Hence, a value of 20 for I_{CT}^{max} is adopted based on a number of industrial catalogues [14]. Better design and core material of the CT allow measuring higher currents accurately and therefore, faster tripping time and better optimization. Moreover, the upper limits for the primary relay operating time and the backup relay operating time are expressed in (9). The proposed protection coordination optimization algorithm is shown in Fig. 2.

The test system is divided into protection zones and the relays zones are assigned manually. The fault currents and load currents observed by each relay are calculated accordingly, and fed to the optimization software. For each protection relay, the software detects the size of fault current for all types of faults observed by the concerned relay. This includes double phase faults, and fault current in the backup protection zone to determine I_p , while the three phase fault is used to determine TDS primary, and TDS backup. The minimum pickup current for the relay is determined as 110% of the largest load current experienced by the relay. At the same time, the maximum pickup current for the relay is set to be 60% of the smallest fault current observed by the relay. The software verifies that the upper limit of the pickup current is higher than the lower limit:

$$110\% \times I_{load} \leq 60\% \times \min \{I_{fault}\}$$

If this criterion could not be satisfied, the upper limit is relaxed to 80% of the lowest fault current. The software proceeds to start the optimization algorithm using the PSO algorithm to find the optimal relays settings; I_p , TDS primary, and TDS backup according to constraints in (4), (5), and (6). The optimization problem is repeated 50 times in order to find the best possible solution, and eliminate local optima.

III. DESCRIPTION OF THE TEST SYSTEM

The proposed protection settings algorithm is tested on a distribution portion of the IEEE 30 Bus test system. The test system is modeled based on the parameters given in the appendix according to [26]. The test system consists of 3 distribution substations with 132/33 kV, 50 MVA transformers, 14 buses and 16 feeders. Bolted three phase faults are tested at the midpoint of lines at nodes {F15 - F30} represent the fault position at the midpoint of lines. Synchronous based distributed generation are distributed at some feeders as shown in Fig. 3. The Distributed Generators (DGs) rating are selected so that it can supply the local load in case of islanded operation mode. The DGs operate step up transformers 6.6/33 kV. The distributed generators and the step-up transformers parameters are given in Appendix.

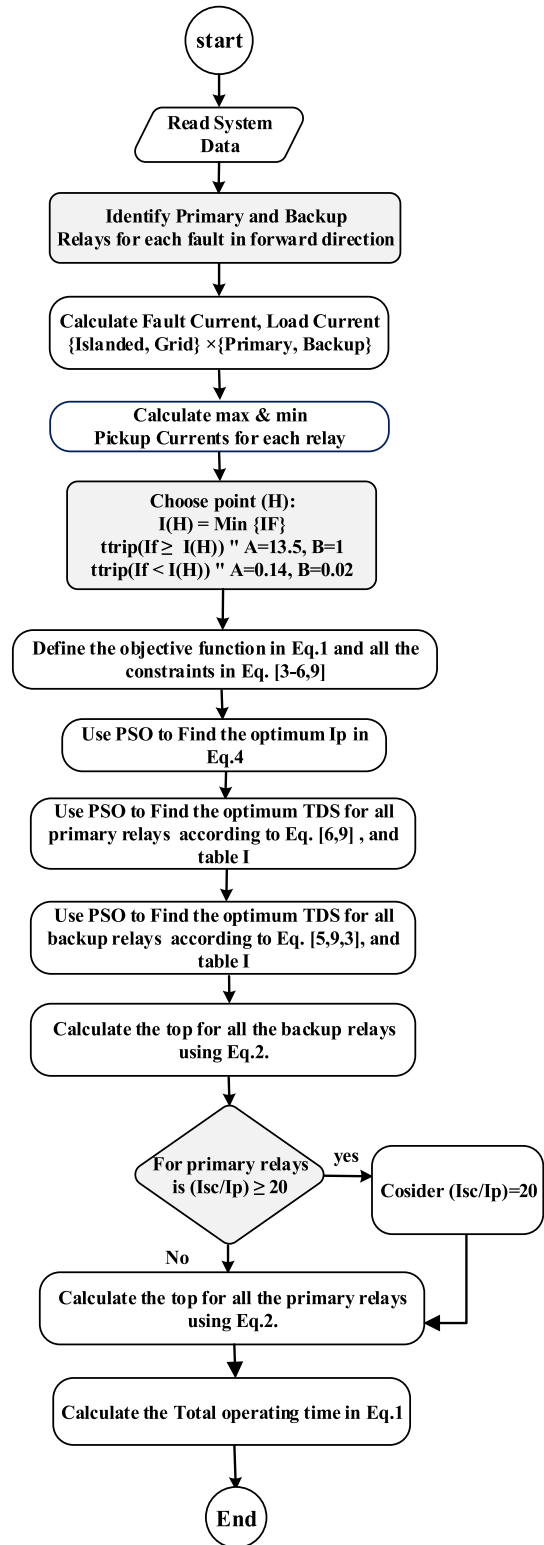


Fig. 2. The proposed optimization protection technique.

The optimal coordination is executed to determine optimal relay settings valid for both modes of operation (grid-connected and islanded). In the grid-connected mode, the test system is supplied through the substation at buses 2, 8 and 12 and the DGs. In case of islanded mode of operation, the DGs can

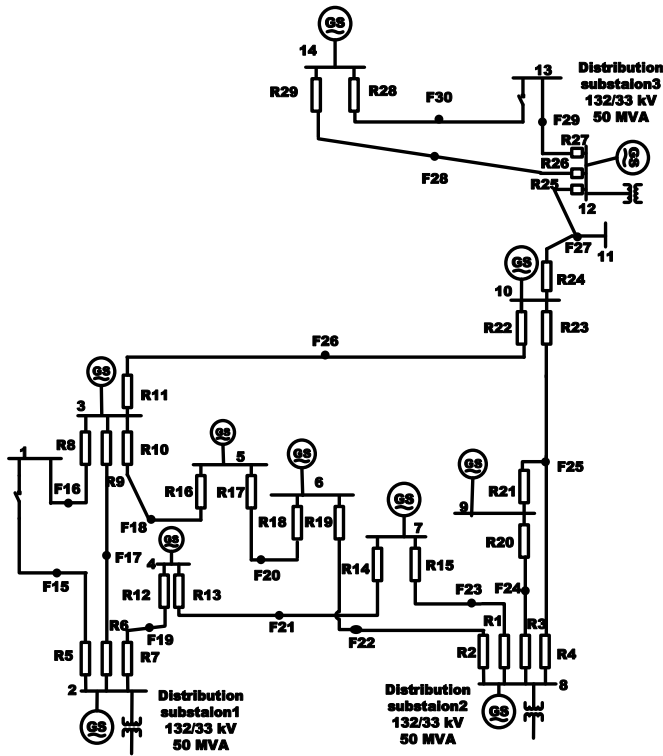


Fig. 3. The distribution portion of the IEEE 30 bus system [18], [19], [25].

feed all the local loads. The protection coordination algorithm includes multi subroutine, which executed in MATLAB. The first one determines the load current in case of islanded and grid-connected mode of operation. The second one determines the fault current for both primary and backup relays in islanded and grid-connected modes of operation. In the last subroutine for optimization, particle swarm optimization (PSO) algorithm is used to produce the protection settings. PSO is one of the heuristic optimization algorithms that deals with a continuous solution space. Each decision variable is represented by one coordinate in a vector. The position and speed are updated for each dimension independently; that is, without interference from any other dimensions [27]. Therefore, the authors believe that PSO is the more suitable tool to solve this problem.

IV. SIMULATION RESULTS AND ANALYSIS

The single point coordination strategy which is adopted in [18] is used here in both methods; the proposed method and the benchmark method [18]. In this section the optimized relays setting, and total operating time for faults at midpoint {F15 - F30} are discussed. The dual-setting design method introduced in [18] is applied on the modified test system shown in Fig. 3 for the comparative analysis and evaluation. The settings of both design techniques are tested in both grid-connected and islanded modes of operation as follows:

A. Performance based on Single Point Coordination Strategy

The same portion of the test system presented in [18] is used in this paper. In order to hold an objective and fair comparison between the two protection design techniques, the proposed optimization protection technique shown in Fig. 2 is compared with the dual setting method in ref [18] for both grid-connected and islanded modes of operation with DG's connection.

1) *The Dual Setting Optimization Method in Ref. [18]*: The dual setting optimization protection method in ref [18] involves four protection settings (TDS_i^b , I_p^{bk} , TDS_i^p , I_p^p) for the DOCRs, which are valid for (grid connected and islanded) operation modes. Each relay has a TDS for primary protection which operates in the forward direction and another TDS for backup protection which operates in reverse direction. The used objective function is the same one in Eq. (1), the result operating time for the protection relays will follow Eq. (2). The used constraints in [18] are:

$$CTI = 0.3 \text{ s.}$$

$$TDS_{\min} \leq TDS_i^{bk} \leq TDS_{\max}$$

$$TDS_{\min} \leq TDS_i^{pm} \leq TDS_{\max}$$

TDS_{\max} and TDS_{\min} are the upper and lower limits of a relay's TDS. A TDS_{\min} value of 0.1 s is adopted here, in accordance with the design parameters of [18], and $TDS_{\max} = 3.2$.

The protection curve used in [18] is the normal inverse curve for both primary and backup settings. The corresponding values for parameters A and B in Eq. (2) are 0.14, and 0.02, respectively. The minimum and maximum operating times are 0.1 s, and 2.5 s, respectively. The optimum protection settings obtained are implemented on the selected test system and tested also with a different set of scenarios for faults occurring at the midpoint of transmission lines, as depicted by Fig. 2. Tables II and III represent the detailed results of primary and backup relays operating time in case of faults {F15-F30} in islanded mode and grid connected mode respectively. It can be seen from the results; the coordination is preserved between primary and backup relays with respect to CTI. While the minimum and maximum limits for the operating time are maintained also.

Eq. (10) is used here, for I_{CT}^{max} value = 20; to demonstrate the validity of the obtained results in a real-world industrial application. The primary relays operating time is almost 0.2267 s. This is because the fault current in the primary relays is relatively high ($I_f/I_p \geq 20$). As a result, the operating time cannot be less than 0.2267 s with the lowest $TDS = 0.1$. It is difficult to improve the operating time for the primary relays beyond these values. For backup relays operating time, the smallest value theoretically possible is around 0.5287 s, which corresponds to a tripping time of 0.2267 for the primary protection relay, and a CTI of 0.3 s. The actual results for backup relays operating time vary between 0.5287 s and 1.0191 s. These values vary between islanded to grid-connected modes, as well. This is because the fault current observed by the relays vary between the two modes of operation.

TABLE II
RELAYS OPERATING TIMES USING PROTECTION SCHEME IN [18]
(ISLNADED OPERATION)

Fault location	Operating times of relays in sec (p=primary, b=backup)			
	P	b1	b2	b3
F15	R5	R6	R7	-
	0.2267	0.5680	0.6230	-
F16	R8	R9	R10	R11
	0.2267	0.9177	0.6262	0.6258
F17	R6	R7	-	-
	0.2267	0.5287	-	-
	R9	R10	R11	-
	0.2267	0.5287	0.5312	-
F18	R10	R9	R11	-
	0.2267	0.5917	0.6010	-
	R16	R17	-	-
	0.2286	0.5287	-	-
F19	R7	R6	-	-
	0.2267	0.5287	-	-
	R12	R13	-	-
	0.2267	0.5397	-	-
F20	R17	R16	-	-
	0.2267	0.5408	-	-
	R18	R19	-	-
	0.2267	0.5287	-	-
F21	R13	R12	-	-
	0.2267	0.5287	-	-
	R14	R15	-	-
	0.2267	0.5287	-	-
F22	R2	R1	R3	R4
	0.2267	0.7646	0.6867	0.8612
	R19	R18	-	-
	0.2267	0.5287	-	-
F23	R1	R2	R3	R4
	0.2267	0.5287	0.5287	0.5287
	R15	R14	-	-
	0.2267	0.5291	-	-
F24	R3	R1	R2	-
	0.2267	0.5287	0.5287	-
	R20	R21	-	-
	0.2267	0.5532	-	-
F25	R4	R1	R2	-
	0.2267	0.5389	0.5287	-
	R21	R20	-	-
	0.2267	0.5287	-	-
	R23	R22	R24	-
	0.2267	0.5502	0.5990	-
F26	R11	R9	R10	-
	0.2267	0.7266	0.7410	-
	R22	R23	R24	-
	0.2267	0.5419	0.7557	-
F27	R24	R22	R23	-
	0.2267	0.6889	0.5897	-
	R25	R26	-	-
	0.2268	0.5287	-	-
F28	R26	R25	-	-
	0.2267	0.5837	-	-
	R29	-	-	-
	0.2267	-	-	-
F29	R27	R25	R26	-
	0.2267	0.5311	0.5522	-
F30	R28	R29	-	-
	0.2267	0.5415	-	-

TABLE III
RELAYS OPERATING TIMES USING PROTECTION SCHEME IN [18]
(GRID-CONNECTED OPERATION)

Fault location	Operating times of relays in sec (p=primary, b=backup)			
	P	b1	B2	B3
F15	R5	R6	R7	-
	0.2267	0.6845	0.7016	-
F16	R8	R9	R10	R11
	0.2267	0.6693	0.6525	0.6445
F17	R6	R7	-	-
	0.2267	0.5520	-	-
	R9	R10	R11	-
	0.2267	0.5335	0.5287	-
F18	R10	R9	R11	-
	0.2267	0.5287	0.6192	-
	R16	R17	-	-
	0.2267	0.5291	-	-
F19	R7	R6	-	-
	0.2267	0.6153	-	-
	R12	R13	-	-
	0.2267	0.5287	-	-
F20	R17	R16	-	-
	0.2267	0.5287	-	-
	R18	R19	-	-
	0.2267	0.5287	-	-
F21	R13	R12	-	-
	0.2267	0.5287	-	-
	R14	R15	-	-
	0.2267	0.5287	-	-
F22	R2	R1	R3	R4
	0.2267	0.8331	0.7786	1.0191
	R19	R18	-	-
	0.2267	0.5287	-	-
F23	R1	R2	R3	R4
	0.2267	0.5287	0.5287	0.5487
	R15	R14	-	-
	0.2267	0.5287	-	-
F24	R3	R1	R2	-
	0.2267	0.5287	0.5287	-
	R20	R21	-	-
	0.2267	0.5287	-	-
F25	R4	R1	R2	-
	0.2267	0.5577	0.5287	-
	R21	R20	-	-
	0.2267	0.5287	-	-
	R23	R22	R24	-
	0.2267	0.5287	0.5287	-
F26	R11	R9	R10	-
	0.2267	0.6184	0.7857	-
	R22	R23	R24	-
	0.2267	0.5287	0.7008	-
F27	R24	R22	R23	-
	0.2267	0.6724	0.5683	-
	R25	R26	-	-
	0.2267	0.5509	-	-
F28	R26	R25	-	-
	0.2267	0.6131	-	-
	R29	-	-	-
	0.2267	-	-	-
F29	R27	R25	R26	-
	0.2267	0.5287	0.5735	-
F30	R28	R29	-	-
	0.2267	0.5287	-	-

TABLE IV
RELAYS SETTING FOR THE OPTIMIZATION IN REF [18]

Relay	Ip primary	TDSprimary	Ip backup	TDS
1	0.118443	0.1	0.118360	0.2332
2	0.005296	0.1	0.009382	0.2332
3	0.074764	0.1	0.073370	0.2332
4	0.034662	0.1	0.070526	0.2114
5	0.068629	0.1	0.202571	0.9046
6	0.211956	0.1	0.212238	0.1635
7	0.106839	0.1	0.081290	0.2332
8	0.119307	0.1	0.070997	0.1286
9	0.211818	0.1	0.211644	0.1720
10	0.056580	0.1	0.130814	0.2009
11	0.069743	0.1	0.068999	0.2043
12	0.098822	0.1	0.087352	0.2332
13	0.125923	0.1	0.149173	0.2003
14	0.108588	0.1	0.103730	0.2332
15	0.126555	0.1	0.128780	0.2332
16	0.048831	0.1	0.555359	0.1007
17	0.052664	0.1	0.163670	0.1878
18	0.054089	0.1	0.053149	0.2332
19	0.020020	0.1	0.074240	0.2332
20	0.080543	0.1	0.073438	0.2332
21	0.272200	0.1	0.293496	0.1680
22	0.057395	0.1	0.061043	0.1827
23	0.113782	0.1	0.065529	0.2077
24	0.050402	0.1	0.142320	0.1066
25	0.110771	0.1	0.095512	0.1204
26	0.026063	0.1	0.025875	0.2223
27	0.030153	0.1	0.952619	3.0603
28	0.111070	0.1	0.030185	0.1192
29	0.025584	0.1	0.149516	0.1015

For example, when fault F22 occurs in islanded operation mode, the backup relay R4 operation time is 0.8612 s.

This time increases to 1.0191 s in case of grid-connected operation mode because the fault current observed by relay R4 is much lower in grid-connected mode. At the same time, other relays demonstrate faster tripping times in grid-connected mode due to higher fault current. For example, when fault F16 occurs in islanded mode, the backup relay R9 operating time is 0.9177. This operating time decreases to 0.6693 in grid-connected operation mode. The optimum relay setting for this method is given in Table IV.

2) *Proposed Dual Setting Optimization Method*: In this section, the results from the proposed protection coordination method will be represented, in addition to comparison between it and the protection method results for [18]. The proposed protection technique produces three protection settings (TDS_i^p ,

TABLE V
COMPARISON BETWEEN THE OPTIMAL TOTAL RELAYS OPERATION TIME IN [18] AND THE PROPOSED PROTECTION COORDINATION SCHEME

Operation Mode	Benchmark method [18]	Proposed scheme	Percentage reduction
All Modes	65.24s	27.98s	57%
Grid-connected Mode	32.70s	13.88s	58%
Islanded operation Mode	32.54s	14.10s	57%

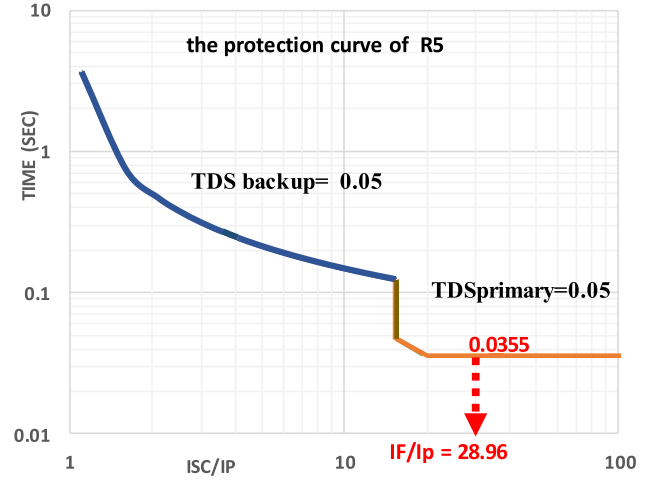


Fig. 4. The protection curve for R5; Primary relay for F15.

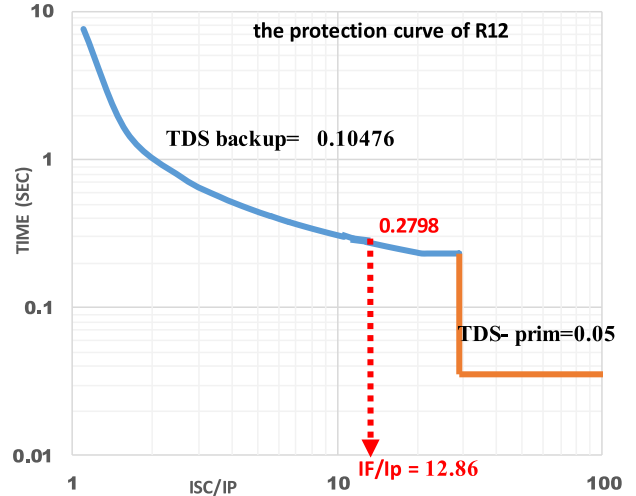


Fig. 5. The protection curve for R9; Backup relay for F15.

TDS_i^p , I_p). The obtained results show that the total relays operating time from the proposed method is reduced significantly from 65.24 s for the method in [18] to 27.98 s, which represents a 57% improvement. Table V presents the relays total operating time in both of the grid-connected and islanded modes along with the improvement margin over the design technique of [18]. The following figures; from Fig. 4 to Fig. 6 represent coordination charts between primary relay and backup relays for F15. In this case the primary relay is R5, while the backup relays are R12 and R9. For the three phase fault at midpoint, the IF/I_p for the primary relay R5 = 28.96, which gives operating time = 0.0355 sec, as indicated in Fig. 4 for the same fault. The backup relay R12, for the same fault, $IF/I_p = 12.86$, which gives time =

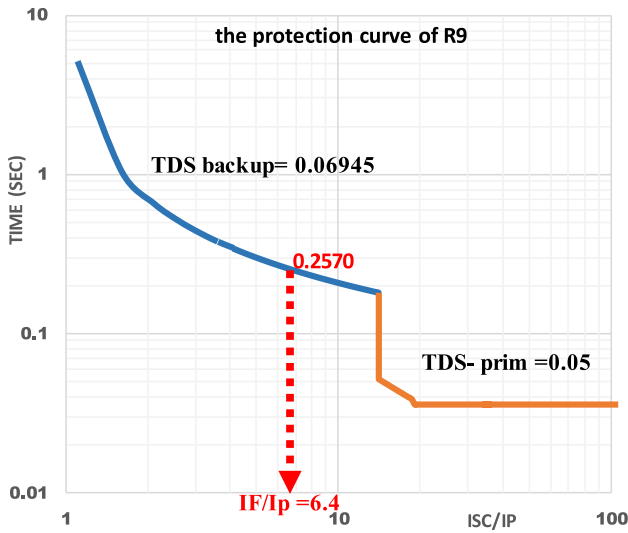


Fig. 6. The protection curve for R12; Backup relay for F15.

0.2789 sec in Fig. 5 while for the other backup relay R9, $IF/I_p = 6.4$ gives time = 0.257 sec, as represented in Fig. 5. It can be concluded that, in these relays set, the coordination time interval (CTI) is maintained.

Furthermore, Table VI illustrates the detailed relays operating time in case of islanded mode. It can be observed that, the minimum coordination time between backup and primary relays is maintained in all fault locations. Moreover, the minimum coordination time interval between primary and backup relays is preserved, along with the maximum operating time constraints enforced upon primary and backup relays. The proposed protection coordination technique demonstrates a significant advantage over the results illustrated in Table II. The majority of primary relays have an operating time of 0.0355 s in Table VI compared with 0.2267 s in Table II. It can be seen that adopting the very inverse curve in primary relays setting improves the primary relays operating time, despite implementing the I_{CT}^{max} constraint. Before comparing the backup protection tripping times for the proposed and the benchmark methods, the following points must be kept in mind: backup protection tripping times for the proposed and the benchmark methods, the following points must be kept in mind: The backup relays operation for the proposed protection technique is in the forward direction, while in Tables II and III the backup relays are in the reverse direction. The minimum backup relays time in Tables II and III is 0.5287s, which is the best time achieved by the benchmark method [18]. Therefore, the comparison between the two methods will consider the values above this one. It can be noticed from the results in Table VI that the proposed protection scheme significantly reduces the backup relays operating times as follows:

- For fault F15, relays R9 and R12 will operate in backup mode after 0.2570 s, and 0.2799 s, respectively to isolate the fault, if relay R5 fails to operate. In the benchmark method, the reverse direction relays, R6 and R7 in Table II operate in 0.5680 s, and 0.6230 s, respectively.
- For fault F16, relays R6, R16, and R22 will operate in the backup mode in 0.4391 s, 0.2375 s, 0.2651 s, respectively.

TABLE VI
RELAYS OPERATING TIMES USING PROPOSED DUAL SETTING PROTECTION SCHEME (ISLANDED OPERATION)

Fault location	Operating times of relays in sec (p=primary, b=backup)			
	p	b1	b2	b3
F15	R5	R9	R12	-
	0.0355	0.2570	0.2799	-
F16	R8	R6	R16	R22
	0.0355	0.4391	0.2375	0.2651
F17	R6	R12	-	-
	0.0355	0.2375	-	-
F18	R9	R16	R22	-
	0.0355	0.2375	0.2375	-
F19	R10	R6	R22	-
	0.0355	0.2824	0.2564	-
F20	R16	R18	-	-
	0.0355	0.2375	-	-
F21	R7	R9	-	-
	0.0355	0.2375	-	-
F22	R12	R14	-	-
	0.0355	0.2417	-	-
F23	R17	R10	-	-
	0.0355	0.2375	-	-
F24	R18	R2	-	-
	0.0355	0.2375	-	-
F25	R13	R7	-	-
	0.0355	0.2375	-	-
F26	R14	R1	-	-
	0.0355	0.2456	-	-
F27	R2	R15	R20	R23
	0.1002	0.2355	0.2356	0.3706
F28	R19	R17	-	-
	0.0355	0.2375	-	-
F29	R1	R19	R20	R23
	0.0355	0.2375	0.2375	0.2375
F30	R15	R13	-	-
	0.0355	0.2439	-	-
F31	R3	R15	R19	R23
	0.0355	0.2375	0.2375	0.2375
F32	R20	R23	R4	-
	0.0355	0.2375	0.3325	--
F33	R4	R15	R19	-
	0.0355	0.2599	0.2375	-
F34	R21	R3	-	-
	0.0355	0.2375	-	-
F35	R23	R11	R25	-
	0.0355	0.2501	0.2586	-
F36	R11	R6	R16	-
	0.0355	0.3459	0.2383	-
F37	R22	R4	R21	R25
	0.0355	0.3950	0.2375	0.2911
F38	R24	R4	R11	R21
	0.0374	0.4664	0.3138	0.2375
F39	R25	R29	-	-
	0.0355	0.2375	-	-
F40	R26	R24	-	-
	0.0355	0.2538	-	-
F41	R29	-	-	-
	0.0355	-	-	-
F42	R27	R24	R29	-
	0.0355	0.2375	0.2502	-
F43	R28	R26	-	-
	0.0355	0.2402	--	-

With the benchmark method, R9, R10, R11 in Table II take relatively longer times to operate 0.9177 s, 0.6262 s, and 0.6258 s, respectively.

- For fault F18, when relay R10 fails to operate, R6, and R22 operate in 0.2824 sec, and 0.2564 s, respectively. With the benchmark method, R9, and R11 in Table II operate in 0.5917 s, 0.6010 s, respectively.

- For F22, the backup relays R15, R20, and R23 operate fast if R2 fail in time 0.2355 s, 0.2356 s, and 0.3706 s, respectively, while in Table II the backup relays R1, R3, and R4 took long time to operate 0.7646 sec, 0.6867 sec, and 0.8612 respectively in Table II.
- For F25, R25 is one of backup relays in case of R23 does not operate in 0.2586 s, instead of R24 in the reverse direction with slower operating time 0.5990 s in Table II.
- For further results analysis, in case of F26, if R11 fails to operate, R6 and R16 will operate in 0.3459 s, and 0.2383 s, respectively instead of R9 and R10 which operated slower in 0.7266 s, 0.7410 s, respectively in Table II. For the same fault, if R22 fails to operate, the backup relays R4, R21, and R25 will operate in time 0.3950 s, 0.2375 s, and 0.2911 s, instead of R23, and R24, which operate in 0.5419 s, and 0.7557 s in Table II.
- For F27, if R24 does not operate, the backup R4, R11, and R21, will operate fast in 0.4664 s, 0.3138 s, and 0.2375 s, respectively, instead of R22, and R23 with slower operating time 0.6889 s, and 0.5897 s in Table II.
- For F28, R24 operate fast to isolate fault in case of R26 fails in 0.2538 s, instead of R25 in reverse direction which operate slower in 0.5837 s in Table II.
- For F29, R29 operate fast to isolate fault in case of R27 fails in 0.2502 s, instead of R26 in reverse direction which operate slower in 0.5522 s in Table II.
- For F30, R26 operate fast to isolate fault in case of R28 fails in 0.2402 s, instead of R29 in reverse direction which operate slower in 0.5415 s in Table II.

For the grid-connected operation mode, Table VII presents the detailed relays operating time for the proposed method. It can be observed that the coordination between backup and primary relays is maintained in all fault locations. The maximum operating time conditions are kept for the primary and backup relays. The primary relays operating time in Table VII are much enhanced than in Table III. The primary relays operating times values are 0.0355 s, while in Table III, it was 0.2267 s. All backup relays operating times are enhanced compared to those in Table III as follows:

- In case of F15, R9, and R12 are the backup relays for R5 with operating time 0.3137 s, and 0.3152 s, instead of R6, and R7 in reverse direction protection in Table III, which have slow operating time 0.6845 s, and 0.7016 s.
- For F16, in case the primary relay R8 does not work, the backup relays R6, R16, and R22 work fast to isolate the fault in 0.2619 s, 0.2375 s, and 0.2814 s, respectively. While the backup relays in reverse direction in Table III, R9, R10, and R11 operated slower to clear the fault in 0.6693 s, 0.6525 s, and 0.6445 s, respectively.
- For F17, R12 operate fast in 0.2503 s, in case of R6 fails, instead of R7 in Table III which operate slower in 0.5520 s.
- For F18, R22 is one of the backup relays for R10, which operates in 0.2591 s, instead of waiting long time for R11 in Table III to operate in 0.6192 s.
- For F19, R9 is the responsible relay to clear the fault in case the main relay R7 has mal-operation in time 0.2618 s,

TABLE VII
RELAYS OPERATING TIMES USING PROPOSED DUAL SETTING PROTECTION SCHEME (GRID-CONNECTED OPERATION)

Fault location	Operating times of relays in sec (p=primary, b=backup)			
	p	b1	b2	b3
F15	R5	R9	R12	-
	0.0355	0.3137	0.3152	-
F16	R8	R6	R16	R22
	0.0355	0.2619	0.2375	0.2814
F17	R6	R12	-	-
	0.0355	0.2503	-	-
	R9	R16	R22	-
F18	0.0355	0.2375	0.2375	-
	R10	R6	R22	-
	0.0355	0.2375	0.2591	-
F19	R16	R18	-	-
	0.0355	0.2375	-	-
	R7	R9	-	-
F20	0.0355	0.2618	-	-
	R12	R14	-	-
	0.0355	0.2375	-	-
F21	R17	R10	-	-
	0.0355	0.2375	-	-
	R18	R2	-	-
F22	0.0355	0.2375	-	-
	R13	R7	-	-
	0.0355	0.2375	-	-
F23	R14	R1	-	-
	0.0355	0.2375	-	-
	R2	R15	R20	R23
F24	0.0355	0.4389	0.4946	0.4205
	R19	R17	-	-
	0.0355	0.2375	-	-
F25	R1	R19	R20	R23
	0.0355	0.2375	0.2483	0.2437
	R15	R13	-	-
F26	0.0355	0.2375	-	-
	R3	R15	R19	R23
	0.0355	0.2426	0.2375	0.2375
F27	R20	R23	R4	-
	0.0355	0.2375	0.2375	-
	R4	R15	R19	-
F28	0.0355	0.2705	0.2375	-
	R21	R3	-	-
	0.0355	0.2375	-	-
F29	R23	R11	R25	-
	0.0355	0.2375	0.2375	-
	R11	R6	R16	-
F30	0.0355	0.2943	0.2472	-
	R22	R4	R21	R25
	0.0355	0.3306	0.2375	0.2783
F31	R24	R4	R11	R21
	0.0355	0.3652	0.3015	0.2375
	R25	R29	-	-
F32	0.0355	0.2492	-	-
	R26	R24	-	-
	0.0355	0.2706	-	-
F33	R29	-	-	-
	0.0355	-	-	-
	R27	R24	R29	-
F34	0.0355	0.2462	0.2636	-
	R28	R26	-	-
	0.0355	0.2375	-	-

instead of waiting time 0.6153 s for R6 in Table III to operate.

- In case of F22, the backup relays R15, R20, and R23 for R2 will operate in time 0.4389 s, 0.4946 s, and 0.4205 s, respectively, instead of R1, R3 and R4 in the reverse direction in Table III with very long operating times 0.8331 s, 0.7786 s, and 1.0191 s, respectively.

TABLE VIII
OPTIMAL RELAYS SETTINGS FOR THE PROPOSED DUAL SETTINGS

relay	Ip (p.u)	TDS (primary)	TDS (backup)
1	0.190703	0.05	0.0998
2	0.059294	0.05	0.1048
3	0.162782	0.05	0.1048
4	0.070533	0.05	0.0710
5	0.160438	0.05	0.0500
6	0.212222	0.05	0.0818
7	0.090897	0.05	0.1048
8	0.070970	0.05	0.3497
9	0.238887	0.05	0.0695
10	0.052647	0.05	0.1048
11	0.071498	0.05	0.0781
12	0.081290	0.05	0.1048
13	0.118293	0.05	0.1027
14	0.112511	0.05	0.0999
15	0.176431	0.05	0.0968
16	0.042570	0.05	0.1048
17	0.082819	0.05	0.1048
18	0.060497	0.05	0.1048
19	0.031757	0.05	0.1048
20	0.165845	0.05	0.0883
21	0.024661	0.05	0.1048
22	0.044770	0.05	0.1048
23	0.065010	0.05	0.1048
24	0.062372	0.05	0.0709
25	0.065767	0.05	0.0776
26	0.031923	0.05	0.1002
27	0.101575	0.05	0.0503
28	0.029332	0.05	0.0501
29	0.039071	0.05	0.0851

TABLE IX
H-POINTS SETTINGS IN RELAYS

relay	H setting	relay	H setting
1	27.81	15	20.03
2	40.87	16	56.32
3	28.38	17	38.29
4	11.81	18	50.77
5	15.45	19	63.98
6	15.65	20	16.61
7	29.63	21	80.98
8	34.98	22	30.69
9	14.04	23	27.06
10	49.28	24	8.91
11	20.25	25	12.19
12	28.77	26	35.65
13	20.01	27	15.61
14	25.20	28	44.90
29	25.74		

TABLE X
OPTIMAL RELAYS SETTING FOR PROPOSED METHOD FOR THREE-POINT COORDINATION STRATEGY

Relay	Ip (p.u)	TDS (primary)	TDS (backup)
1	0.184141	0.05	0.104375
2	0.089984	0.05	0.117012
3	0.164869	0.05	0.104833
4	0.070510	0.05	0.104057
5	0.176016	0.05	0.336965
6	0.211640	0.05	0.105083
7	0.089474	0.05	0.106167
8	0.110208	0.05	0.052504
9	0.211644	0.05	0.103219
10	0.051972	0.05	0.108441
11	0.069041	0.05	0.104518
12	0.081964	0.05	0.106892
13	0.107691	0.05	0.105919
14	0.105244	0.05	0.114090
15	0.176537	0.05	0.104328
16	0.042570	0.05	0.106412
17	0.052160	0.05	0.201878
18	0.060722	0.05	0.108975
19	0.032994	0.05	0.110239
20	0.162709	0.05	0.104860
21	0.021279	0.05	0.108165
22	0.045230	0.05	0.105101
23	0.066477	0.05	0.105511
24	0.050380	0.05	0.106987
25	0.061139	0.05	0.106680
26	0.030931	0.05	0.111429
27	0.045540	0.05	0.089856
28	0.031312	0.05	0.334296
29	0.028378	0.05	0.112188

- For F26, R6, and R16 are the backup relays for R11, which operate fast in 0.2943 s, and 0.2472 s, respectively, while the backup relays R9, and R10 in Table III took long time to operate 0.6184 s, and 0.7857 s, respectively.
- For the same fault location F26, R25 is one of the backup relays for R22 which operate fast in 0.2783 s to isolate the fault, instead of R24 in the reverse direction in Table III which operated in 0.7008 s.
- For F27, R4, R11, and R21 are the backup relays for R24, which operate fast to clear the fault in 0.3652 s, 0.3015 s, and 0.2375 s, instead of R22, and R23, which take longer time to operate in 0.6724 s, and 0.5683 s in Table III.
- For the same fault F27, R29 is a backup for R25 in time 0.2492 s, instead of R26, which operates slower in time 0.5509 s in Table III.
- For F28, if R26 fails to operate, R24 will operate fast in 0.2706 s, instead of R25 in Table III, which operate in 0.6131 s.
- For F29, R29 will operate as a backup to isolate fault in case of R27 fails to trip in time 0.2636 s compared to backup relay R26 in Table III, which operated in 0.5735 s.

Table VIII gives the proposed relays settings, which achieve the reduction in relays operation time and maintain the proper

coordination between backup and primary relays. Table IX represents the setting of H points in all relays.

B. Performance Based on Three-Point Coordination Strategy

In this section the proposed dual setting optimization method will be implemented through the three-point coordination strategy on the test system. The three-point coordination strategy is more accurate and reliable more than the single point coordination strategy [16]–[22]–[23]. The relays coordination in this strategy will be based on three points for faults on the protected

TABLE XI
OPTIMAL RELAYS SETTINGS FOR REF [18] FOR THREE-POINT
COORDINATION STRATEGY

Relay	Ip primary	TDSprimary	Ip backup	TDS
1	0.207966	0.1	0.118360	0.232367
2	0.174870	0.1	0.029835	0.232367
3	0.191064	0.1	0.074347	0.232367
4	0.093738	0.1	0.070512	0.232358
5	0.083770	0.1	1.605453	0.149354
6	0.211668	0.1	0.211641	0.226973
7	0.110794	0.1	0.081301	0.232317
8	0.232198	0.1	0.074005	0.668574
9	0.211640	0.1	0.211643	0.232320
10	0.075308	0.1	0.049980	0.235216
11	0.151641	0.1	0.068675	0.232320
12	0.083253	0.1	0.081325	0.232326
13	0.149589	0.1	0.103913	0.232351
14	0.183416	0.1	0.103741	0.232687
15	0.129163	0.1	0.174402	0.232317
16	0.043417	0.1	0.071824	0.232318
17	0.162988	0.1	0.052392	0.232317
18	0.173883	0.1	0.052142	0.232318
19	0.117462	0.1	0.034789	0.232318
20	0.246497	0.1	0.073405	0.264783
21	0.255205	0.1	0.032969	0.232807
22	0.056516	0.1	0.044770	0.232320
23	0.071483	0.1	0.067039	0.236851
24	0.066730	0.1	0.050409	0.240143
25	0.082525	0.1	0.061050	0.232317
26	0.032008	0.1	0.024090	0.232319
27	0.100384	0.1	0.858450	0.410087
28	0.041422	0.1	0.749015	0.107164
29	0.087752	0.1	0.024090	0.232426

TABLE XII
TOTAL RELAYS TRIPPING TIME IN CASE OF NEAR END, MIDPOINT, FAR END
FAULT FOR THE PROPOSED METHOD AND REF [18] METHOD

Fault location	Operation mode	Benchmark method [18]	Proposed scheme	Percentage reduction
Near end Fault	All Modes	70.26	32.75	53%
	On-grid Mode	35.10	14.42	59%
	Islanded-Mode	35.16	18.33	48%
Midpoint Fault	All Modes	77.27	33.56	57%
	On-grid Mode	38.70	17.19	56%
	Islanded-Mode	38.57	16.37	58%
Far end Fault	All Modes	100.62	41.37	59%
	On-grid Mode	50.14	21.73	57%
	Islanded-Mode	50.48	19.64	61%
Total time for near end, midpoint, fare end faults		248.15	107.68	57%

lines; near end fault, midpoint fault, and far end fault. The three-point coordination strategy is also implemented for the benchmark method [18], in order to compare the results.

Table X shows the new optimization relays settings for the proposed method in case of three-point coordination strategy.

Table XI represents the new optimization relays settings for the benchmark method presented in ref [18] in case of three-point coordination strategy. The new settings have been tested successfully in case of near end fault, midpoint fault, and far end fault. Table XII presents a comparison for the total operating time between the proposed method, and benchmark method [18] in case of near end, midpoint, and far end faults. It is clear from Table XII that the proposed method performs better at all fault locations. In fact, the proposed method reduces the total operating time for all fault location by 57%.

V. CONCLUSION

This paper proposes a novel protection coordination method for the direction overcurrent relays settings in microgrids with distributed generation units. The proposed method utilizes a double protection setting for primary and backup operation modes in a single relay. The proposed method is suitable for applications with both islanded and grid-connected operation modes with faster operating time in both modes. The proposed dual setting contributes significant improvement to system reliability, as it eliminates the need for communication among relays. The proposed technique is tested on a modified IEEE test system and the results are discussed. The optimization is executed in case of single point coordination strategy and in case of three-point coordination strategy. The results demonstrate superior performance of the proposed method over the traditional dual setting method by reducing the total operating time of 57% for all fault locations while employing the three-point coordination strategy.

APPENDIX

Parameters of the Distributed Generators

Bus	The generators rating (MVA), 6.6 kV	The generators sub transient reactance (p.u)	Transformer Short circuit Impedance (p.u) (6.6 :33) kV
8	8.35	0.202	0.075
2	9.15	0.202	0.075
3	18	0.154	0.08
4	7.75	0.235	0.075
7	10.4	0.189	0.08
5	5.13	0.166	0.07
6	13.3	0.167	0.08
9	11.25	0.184	0.08
10	15.100	0.174	0.08
12	6.680	0.138	0.075
14	9.9	0.144	0.075

REFERENCES

- [1] V. Telukunta, J. Pradhan, A. Agrawal, M. Singh, and S. G. Srivani, "Protection challenges under bulk penetration of renewable energy resources in power systems: A review," *CSEE J. Power Energy Syst.*, vol. 3, no. 4, pp. 365–379, Dec. 2017.
- [2] X. Xu, J. Mitra, T. Wang, and L. Mu, "An evaluation strategy for microgrid reliability considering the effects of protection system," *IEEE Trans. Power Del.*, vol. 31, no. 5, pp. 1989–1997, Oct. 2016.
- [3] S. M. Sharkh, M. A. Abu-Sara, G. I. Orfanoudakis, and B. Hussain, "Microgrid protection," in *Power Electron. Converters Microgrids*, 1st ed., Wiley, 2014, pp. 221–237.

- [4] A. Oudalov, T. Degner, F. van Overbeeke, and J. M. Yarza, "Microgrid protection," in *Microgrids: Architectures and Control*, 1st ed., Wiley, 2014, pp. 117–164.
- [5] X. Kang, C. E. K. Nuworklo, B. S. Tekpeti, and M. Kheshti, "Protection of micro-grid systems: A comprehensive survey," *J. Eng.*, vol. 2017, no. 13, pp. 1515–1518, 2017.
- [6] A. Hooshyar and R. Irvani, "A new directional element for microgrid protection," *IEEE Trans. Smart Grid*, vol. 9, no. 6, pp. 6862–6876, Nov. 2018.
- [7] A. Y. Hatata and A. Lafi, "Ant lion optimizer for optimal coordination of DOC relays in distribution systems containing DGs," *IEEE Access*, vol. 6, pp. 72241–72252, 2018.
- [8] E. Dehghanpour, H. K. Karegar, R. Kheirollahi, and T. Soleymani, "Optimal coordination of directional overcurrent relays in microgrids by using cuckoo-linear optimization algorithm and fault current limiter," *IEEE Trans. Smart Grid*, vol. 9, no. 2, pp. 1365–1375, Mar. 2018.
- [9] A. Sharma and B. K. Panigrahi, "Phase fault protection scheme for reliable operation of microgrids," *IEEE Trans. Ind. Appl.*, vol. 54, no. 3, pp. 2646–2655, May/June. 2018.
- [10] E. Purwar, D. N. Vishwakarma, and S. P. Singh, "A novel constraints reduction-based optimal relay coordination method considering variable operational status of distribution system with DGs," *IEEE Trans. Smart Grid*, vol. 10, no. 1, pp. 889–898, Jan. 2019.
- [11] A. Y. Hatata *et al.*, "Application of resistive super conductor fault current limiter for protection of grid-connected DGs," *Alexandria Eng. J.*, vol. 57, no. 4, Dec. 2018, pp. 4229–4241.
- [12] H. He *et al.*, "Application of a SFCL for fault ride-through capability enhancement of DG in a microgrid system and relay protection coordination," *IEEE Trans. Appl. Supercond.*, vol. 26, no. 7, pp. 1–8, Oct. 2016.
- [13] D. Saha, A. Datta, and P. Das, "Optimal coordination of directional overcurrent relays in power systems using symbiotic organism search optimisation technique," *IET Gener., Transmiss. Distrib.*, vol. 10, no. 11, pp. 2681–2688, 2016.
- [14] N. El-Naily, S. M. Saad, T. Hussein, and F. A. Mohamed, "A novel constraint and non-standard characteristics for optimal over-current relays coordination to enhance microgrid protection scheme," *IET Gener. Transmiss. Distrib.*, vol. 13, no. 6, pp. 780–793, 2019.
- [15] K. A. Saleh, H. H. Zeineldin, A. Al-Hinai, and E. F. El-Saadany, "Optimal coordination of directional overcurrent relays using a new time-current-voltage characteristic," *IEEE Trans. Power Del.*, vol. 30, no. 2, pp. 537–544, Apr. 2015.
- [16] A. Yazdanejadi, M. S. Naderi, G. B. Gharehpetian, and V. Talavat, "Protection coordination of directional overcurrent relays: New time current characteristic and objective function," *IET Gener., Transmiss. Distrib.*, vol. 12, no. 1, pp. 190–199, 2018.
- [17] M. Lwin, J. Guo, N. B. Dimitrov, and S. Santoso, "Stochastic optimization for discrete overcurrent relay tripping characteristics and coordination," *IEEE Trans. Smart Grid*, vol. 10, no. 1, pp. 732–740, Jan. 2019.
- [18] H. M. Sharaf, H. H. Zeineldin, and E. El-Saadany, "Protection coordination for microgrids with grid-connected and islanded capabilities using communication assisted dual setting directional overcurrent relays," *IEEE Trans. Smart Grid*, vol. 9, no. 1, pp. 143–151, Jan. 2018.
- [19] H. H. Zeineldin, H. M. Sharaf, D. K. Ibrahim, and E. E. A. El-Zahab, "Optimal protection coordination for meshed distribution systems with DG using dual setting directional over-current relays," *IEEE Trans. Smart Grid*, vol. 6, no. 1, pp. 115–123, Jan. 2015.
- [20] T. S. Aghdam, H. Kazemi Karegar, and H. H. Zeineldin, "Optimal coordination of double-inverse overcurrent relays for stable operation of DGs," *IEEE Trans. Ind. Informat.*, vol. 15, no. 1, pp. 183–192, Jan. 2019.
- [21] R. Tiwari, R. K. Singh, and N. Kumar Choudhary, "Optimal coordination of dual setting directional over current relays in microgrid with different standard relay characteristics," in *Proc. IEEE 9th Power India Int. Conf.*, 2020, pp. 1–6.
- [22] K. A. Saleh, H. H. Zeineldin, A. Al-Hinai, and E. F. El-Saadany, "Dual-setting characteristic for directional overcurrent relays considering multiple fault locations," in *IET Gener. Transmiss. Distrib.*, vol. 9, no. 12, pp. 1332–1340, 2015.
- [23] A. Yazdanejadi, S. Golshannavaz, D. Nazarpour, S. Teimourzadeh, and F. Aminifar, "Dual-Setting directional overcurrent relays for protecting automated distribution networks," *IEEE Trans. Ind. Informat.*, vol. 15, no. 2, pp. 730–740, Feb. 2019.
- [24] H. F. Habib, C. R. Lashway, and O. A. Mohammed, "A review of communication failure impacts on adaptive microgrid protection schemes and the use of energy storage as a contingency," *IEEE Trans. Ind. Appl.*, vol. 54, no. 2, pp. 1194–1207, Mar./Apr. 2018.
- [25] SIPROTEC 5. Overcurrent Protection, 7SJ82/7SJ85, technical manual, Nov. 2017. [Online]. Available: <https://new.siemens.com/global/en/products/energy.html>
- [26] University Washington, Power Systems Test Case Archive, Seattle, WA. [Online]. Available: <http://www.ee.washington.edu/research/>
- [27] E. K. Burke and G. Kendall, *Search Methodologies: Introductory Tutorials in Optimization and Decision Support Techniques*. New York, NY, USA: Springer Link, 2005.



Heba Beder was born in Egypt in 1983. She received the B.Sc. and M.Sc. degrees in electrical engineering from Mansoura University, Egypt, in 2005 and 2012, respectively. She is currently working toward the Ph.D. degree with Mansoura University. She is a Protection Engineer with North Delta Electricity Distribution Company, Egypt.

Her research interests include power system protection, distributed generation, and power system automation.



Baraa Mohandes (Member, IEEE) received the B.Sc. degree in electrical engineering (with honors) in 2010 from Khalifa University, the Petroleum Institute, UAE, where he was the recipient of the Abu-Dhabi National Oil Company's (ADNOC) scholarship. Following the B.Sc., he worked as a Technical Support and Projects Engineer in one of ADNOC's subsidiaries in the oil&gas industry from 2010 to 2015. He also completed the M.Sc. degree (with honors) in 2015 from Khalifa University. His research interests include feedback control systems,

optimization, data science, game-theory and power systems. He was the recipient of the Masdar Institute's (MI) fellowship for the joint MI and Massachusetts Institute of Technology (MIT) Program for the Ph.D. in Interdisciplinary Engineering, and received the Ph.D. degree (with Honors and distinction) in 2020 for his work on power systems optimization and economics. Following the completion of the Ph.D., he joined the Luxembourg Institute of Science and Technology (LIST) as a Postdoctoral Associate. He was the recipient of a number of student awards.



Mohamed Shawky El Moursi (Senior Member, IEEE) received the B.Sc. and M.Sc. degrees from Mansoura University, Mansoura, Egypt, in 1997 and 2002, respectively, and the Ph.D. degree from the University of New Brunswick (UNB), Fredericton, NB, Canada, in 2005, all in electrical engineering. He was a Research and Teaching Assistant with the Department of Electrical and Computer Engineering, UNB, from 2002 to 2005. He was with McGill University as a Postdoctoral Fellow with the Power Electronics Group. He joined Vestas Wind Systems,

Arhus, Denmark, in the Technology R&D with the Wind Power Plant Group. He was with TRANSCO, UAE, as a Senior Study and Planning Engineer. He is currently a Professor with the Electrical and Computer Engineering Department, Khalifa University of Science and Technology- Masdar Campus and seconded to a Professor Position in the Faculty of Engineering, Mansoura University, Mansoura, Egypt and currently on leave. He was a Visiting Professor with the Massachusetts Institute of Technology, Cambridge, Massachusetts, USA. His research interests include power system, power electronics, FACTS technologies, VSC-HVDC systems, microgrid operation and control, renewable energy systems (Wind and PV) integration and interconnections. He is currently an Editor for IEEE TRANSACTIONS ON POWER DELIVERY, IEEE TRANSACTIONS ON POWER SYSTEMS, Associate Editor for IEEE TRANSACTIONS ON POWER ELECTRONICS, Associate Editor for IEEE TRANSACTIONS ON SMART GRID, Guest Editor for IEEE TRANSACTIONS ON ENERGY CONVERSION, Guest Editor-in-Chief for special section between TPWRD and TPWRS, Editor for IEEE POWER ENGINEERING LETTERS, Regional Editor for *IET Renewable Power Generation* and Associate Editor for *IET Power Electronics Journals*.



Ebrahim A. Badran (Member, IEEE) was born in Egypt in 1969. He received the B.Sc., M.Sc., and Ph.D. degrees in electrical engineering from Mansoura University, Egypt, in 1991, 1995, and 2004, respectively. From 1993 to 1999, he was an Operation Engineer with the Egyptian Electricity Authority. In 1999, he joined the Academy of Special Studies, Egypt, where he is the Head of Technology Department from 2004 to 2008. He was with the Electrical Engineering Department, University of El-Mansoura, in 2008, where he is currently a Full Professor. His

research interests include transients in power system, power system protection, modeling of power system, power quality, FACTS, and renewable energy.



Magdi M. El Saadawi was born in Mansoura, Egypt, in 1959. He received the B.Sc. and M.Sc. degrees from Mansoura University, Egypt, in 1982 and 1988, respectively, and the Ph.D. degree from the Warsaw University of Technology, in 1997. He was a Teaching Assistant with El-Mansoura University from 1983–1992. From 1997, he was a Staff Member with the Electrical Engineering Department, Mansoura University, and has been a Professor since May 2011. He was the Head with Electrical Engineering Department, Mansoura University from 2011 to 2012. His

research interests include, renewable energy, distributed generation, and power system analysis.